AIDIC CONFERENCE SERIES

VOL. 11, 2013
Chief Editor: Sauro Pierucci

ISBN 978-88-95608-55-6; **ISSN** 2036-5969

A publication of AIDIC
The Italian Association of Chemical Engineering
www.aidic.it/acos

DOI: 10.3303/ACOS1311040

CFD Prediction of Solid Particle Distribution in Baffled Stirred Vessels under Partial to Complete Suspension Conditions

Alessandro Tamburini[a,*], Andrea Cipollina[a], Giorgio Micale[a], Alberto Brucato[a], Michele Ciofalo[b]

[a]Dipartimento di Ingegneria Chimica, Gestionale, Informatica, Meccanica - Università degli Studi di Palermo, Viale delle Scienze Edificio 6 - 90128 Palermo, Italy
[b] Dipartimento dell' Energia, Ingegneria, dell'Informazione e Modelli Matematici - Università di Palermo, Viale delle Scienze Ed. 6, 90128 Palermo, Italy)
alessandro.tamburini@unipa.it

Solid-liquid mixing within tanks agitated by stirrers can be easily encountered in many industrial processes. It is common to find an industrial tank operating at an impeller speed N lower than the minimum agitation speed for the suspension of solid particles: under such conditions the distribution of solid-particles is very far from being homogeneous and very significant concentration gradients exist. The present work evaluates the capability of a Computational Fluid Dynamics (CFD) model to reliably predict the particle distribution throughout the tank under either partial or complete suspension conditions. A flat bottomed baffled tank stirred by a Rushton turbine was investigated. Two different impeller clearances were investigated. Both transient and steady state RANS simulations of the stirred tank were performed with the commercial code CFX4.4®. The Eulerian-Eulerian Multi Fluid Model along with the k-ε turbulence model was adopted. In particular two different versions of this model (homogenous and asymmetric) were tested. Either the Sliding Grid or the Multiple Reference Frame technique was employed to simulate the impeller to baffle relative rotation. Inter-phase momentum exchange terms were approximated only by the inter-phase drag forces. Literature experimental data were used for the model validation. Results show that the model along with the Sliding Grid technique can reliably predict the experimental particle distribution at all investigated impeller speeds. Radial gradients of solids concentration, usually neglected in the literature, where found to be significant in the presence of unsuspended solid particles (partial suspension conditions). Homogenous k-ε turbulence model was found to predict a less intense turbulence resulting into a lower particle distribution degree.

1. Introduction

Industrial tanks devoted to the mixing of solid particles into liquids are often operated at an impeller speed N lower than the minimum one allowing the suspension of particles (N_{js}) (Oldshue, 1983; Rieger et al., 1988; Van der Westhuizen and Deglon, 2007; Jafari et al., 2012; Wang et al., 2012).
Most solid-liquid mixing operations require the knowledge of N_{js} and/or of the amount of solids suspended at different agitation speeds below N_{js} (i.e the suspension curve). In many cases it is also required that information is gained on the quality of the solids distribution within the tank, since the particle distribution may largely affect the process performance. In such cases, a reliable prediction of the solids distribution is of crucial importance for an accurate design and testing of the pertaining solid-liquid stirred systems. Also, the knowledge of local particle concentration fields is essential to allow a sound understanding of the mechanisms of solids suspension and dispersion occurring inside these systems (Tamburini et al., 2013a). Surprisingly, it is not easy to find such data in the literature for partial suspension conditions, notwithstanding the interest expressed so far at the industrial level for this particular regime.

Please cite this article as: Tamburini A., Cipollina A., Micale G., Brucato A., Ciofalo M., 2013, Cfd prediction of solid particle distribution in baffled stirred vessels under partial to complete suspension conditions, AIDIC Conference Series, 11, 391-400 DOI: 10.3303/ACOS1311040

Experimental data on particle distribution into a liquid within a stirred tank are usually presented in the form of axial and radial profiles of solids concentration. In the literature it is easy to find similar local data, especially when the solids concentration is measured by intrusive techniques making use of a probe. Sometimes local information is assumed to be valid for the entire radial direction (Barresi and Baldi, 1987; Shamlou and Koutsakos, 1989; Micheletti et al., 2003) or even for the whole horizontal plane (e.g. this is the case of measurements taken by the light attenuation technique, Magelli et al., 1990). This is justified by assuming that either the radial gradients of solid concentration or both radial and azimuthal gradients are negligible. However, In view of the strongly accelerating and decelerating flows across a stirred vessel, it might be expected that consideration of such gradients may improve the understanding of the suspension performance (Micheletti et al., 2003). The distribution of solid particles in a stirred vessel is a quite complex function of the velocity field, turbulence characteristics and liquid-particle interactions. Thus, the soundness of the former approximation depends on several factors, such as geometrical configuration (Micale et al., 1999) and suspension properties: for example (i) radial impellers provide larger concentration gradients than axial impellers and (ii) the higher the particle size and concentration, the higher the concentration gradients (Barresi and Baldi, 1987).
The present work is devoted to the investigation via CFD of the particle distribution in a dense suspension ranging from partial to complete suspension conditions. In particular, the CFD model by Tamburini et al. (2011a) was purposely developed to deal with partial suspension conditions. It has been fully validated in previous works and found to reliably predict integral data in the form of (i) suspension curves (Tamburini et al., 2011a), (ii) N_{js} (Tamburini et al., 2012a) and (iii) impeller speed for sufficient suspension conditions (Tamburini et al., 2012b). Such essential data concerning the particle suspension phenomenon, however, do not provide any information on local details since they are intrinsically lumped. Investigation of particle distribution completes the description of the solid-liquid suspension by adding a further level of detailed information throughout the whole vessel volume. Here, the model by Tamburini et al. (2011a) is further tested in order to evaluate its capability to deal with local particle concentration distribution under incomplete suspension conditions. Notably, most CFD models proposed in the literature are generally validated against experimental axial profiles of solids concentration collected at N equal or higher than N_{js}.

2. Systems under investigation

The experimental data to be simulated derive from the literature (Micheletti et al., 2003). Only some details are reported in the following, full details can be found in the pertinent paper. The experimental system simulated consisted of a cylindrical flat bottomed baffled tank with vessel diameter T=0.29 m and total liquid height H=T. A standard six-bladed Rushton turbine with diameter D=T/3 was used and set at a distance from the vessel bottom C equal either to 0.15T or to T/3. Deionised water (ρ_α = 1000 kg/m^3) and mono-dispersed glass particles (d_p = 600-710 μm; ρ_β = 2470 kg/m^3) were employed. Solid loading was equal to 9.2% V_{solid}/V_{total} (r_β^{av}). Maximum physically allowed packing value of the particle bed was estimated to be 60% V_{solid}/V_{bed} (r_β^{packed}). These data consist of local steady state axial profiles of solid concentration taken by a conductivity probe at a radial position R/T=0.35, midway between subsequent baffles and at different heights of the tank.

3. Modelling and numerical details

Only a short description of the adopted CFD model will be given in the following; further details can be found in Tamburini et al. (2011a). All CFD simulations were carried out by using the commercial code *CFX4.4* (*Ansys*®). The Eulerian-Eulerian Multi Fluid Model was adopted to simulate the two-phases which are treated as two interpenetrating continua. The relevant continuity and momentum balance equations are reported below.

$$\rho_i \frac{\partial}{\partial t}(r_i) + \rho_i \vec{\nabla} \cdot \left(r_i \vec{U}_i\right) = 0 \qquad (1)$$

$$\frac{\partial}{\partial t}\left(r_i \rho_i \vec{U}_i\right) + \vec{\nabla} \bullet \left\{r_i \left[\rho_i \vec{U}_i \otimes \vec{U}_i - (\mu_i + \mu_t)\left(\vec{\nabla}\vec{U}_i + \left(\vec{\nabla}\vec{U}_i\right)^T\right)\right]\right\} = r_i\left(\rho_i \vec{g} - \vec{\nabla}P\right) + \vec{F}_{i,j} \qquad (2)$$

where r is volumetric fraction, ρ the density and U the mean velocity, i indicates the liquid or solid phase, g the gravity acceleration, μ the viscosity, P the pressure (the solid and the liquid phases share the same pressure field) and F is the inter-phase drag force (clearly $F_{i,j}$=-$F_{j,i}$). All other inter-phase forces were

neglected as suggested by the literature for density ratio between the two phases higher than 2 (Tatterson, 1991). No turbulence was assumed in the solid phase: this choice ("*asymmetric turbulence modelling*") is a specific feature of the model by Tamburini et al. (2011a) and was found suitable to deal with dense solid-liquid suspensions in stirred tanks under partial-to-complete suspension regimes (Tamburini et al., 2011a,b; Tamburini et al., 2012a,b): in particular, the *asymmetric k-ε turbulence model* (Tamburini et al., 2011a) was employed here (equations 3 and 4). A molecular viscosity equal to the liquid one was chosen for the solid phase as suggested by the literature (Tamburini et al., 2011a,b).

$$\rho_\alpha \frac{\partial}{\partial t}(r_\alpha k_\alpha) + \vec{\nabla}\left[r_\alpha \rho_\alpha \vec{U}_\alpha k_\alpha - r_\alpha \left(\mu_\alpha + \frac{\mu_{t\alpha}}{\sigma_k} \right) \vec{\nabla} k_\alpha \right] =$$
$$= r_\alpha \left[\mu_{t\alpha} \vec{\nabla} \vec{U}_\alpha \left(\vec{\nabla} \vec{U}_\alpha + \left(\vec{\nabla} \vec{U}_\alpha \right)^T \right) - \rho_\alpha \varepsilon_\alpha \right] \quad (3)$$

$$\rho_\alpha \frac{\partial}{\partial t}(r_\alpha \varepsilon_\alpha) + \vec{\nabla}\left[r_\alpha \rho_\alpha \vec{U}_\alpha \varepsilon_\alpha - r_\alpha \left(\mu_\alpha + \frac{\mu_{t\alpha}}{\sigma_\varepsilon} \right) \vec{\nabla} \varepsilon_\alpha \right] =$$
$$= r_\alpha \left[C_1 \frac{\varepsilon_\alpha}{k_\alpha} \mu_{t\alpha} \vec{\nabla} \vec{U}_\alpha \left(\vec{\nabla} \vec{U}_\alpha + \left(\vec{\nabla} \vec{U}_\alpha \right)^T \right) - C_2 \rho_\alpha \frac{\varepsilon^2}{k} \right] \quad (4)$$

where $\mu_{t\alpha} = \rho_\alpha C_\mu \frac{{k_\alpha}^2}{\varepsilon_\alpha}$ (5)

C_μ is a constant. For comparison purposes, an alternative to the Tamburini et al. (2011a) turbulence model was tested. In particular also the more common "*homogeneous k-ε turbulence model"* was employed in the present work: in this case the two phases share the same values of k and ε and a turbulent viscosity appears in the momentum equations of both phases. k and ε transport equations remain practically the same with respect to the single-phase case, but no volume fractions are present and all physical properties appearing in these equations are the "mixture" averaged properties. Notably, this *homogeneous k-ε turbulence model* was found to provide a fair representation of the solid distribution throughout the vessel for a number of cases dealing with dense suspensions in stirred tank (Montante et al., 2001; Micale et al., 2004; Montante and Magelli, 2005; Khopkar et al., 2006; Kasat et al., 2008).
A standard formulation was adopted for the drag force:

$$\vec{F}_{\alpha\beta} = \left[\frac{3}{4} \frac{C_D}{d_p} r_\beta \rho_\alpha \left| \vec{U}_\beta - \vec{U}_\alpha \right| \right] \left(\vec{U}_\beta - \vec{U}_\alpha \right) \quad (6)$$

$$C_{D,turb}^{Brucato} = C_{D,slip} \left[1 + 8.76 \times 10^{-4} \left(\frac{d_p}{\lambda} \right)^3 \right] = \left[\frac{24}{\mathrm{Re}_p} \left(1 + 0.2\,\mathrm{Re}_p^{0.63} \right) \right] \left[1 + 8.76 \times 10^{-4} \left(\frac{d_p}{\lambda} \right)^3 \right] \quad (7)$$

where, C_D is drag coefficient. Particle drag coefficient C_D was considered variable in each cell in relation to the slip velocity between phases in accordance with Clift et al. correlation (1978). Free-stream turbulence influence upon drag coefficient was accounted for be employing the correlation by Brucato et al. (1998).
The Excess Solid Volume Fraction Correction (ESVC) algorithm (Tamburini et al., 2009b) was adopted to avoid that r_β^{packed} could be largely exceeded during the simulations.
As far as the treatment of the impeller-baffle relative rotation is concerned, both the steady state Multiple Reference Frame (MRF) and the time dependent Sliding Grid (SG) algorithm (more accurate but much more computationally demanding) were adopted in the present work.
In MRF simulations typically 12000 SIMPLEC iterations were found to be sufficient to allow variable residuals to settle to very low values for all the cases investigated. As far as the SG simulations are concerned, 100 full revolutions were considered sufficient to reach steady state conditions in all cases, coherently with what is reported by the literature for similar systems (Tamburini et al., 2009a and 2011a).

The number of *SIMPLEC* iterations per time step was set to 30 to allow residuals to settle before moving to the next time step.
The *SIMPLEC* algorithm was adopted to couple pressure and velocity. Central differences were employed for all diffusive terms. The quick discretization scheme was employed for the convective terms. In accordance with the system's axial symmetry, only one half of the tank was included in the computational domain and two periodic boundaries were imposed along the azimuthal direction. The structured grid chosen for the discretization of this half-tank encompasses 74592 cells distributed as 72 × 37 × 28 along the axial, radial and azimuthal direction respectively. Some simulations were carried out also by employing a 8 times finer grid: quite identical results (<2% difference in r_β axial profiles) were obtained by employing the two grids.

4. Results and discussion

4.1 Impeller modelling technique

Figure1 reports the comparison between the experimental local profiles of r_β measured by Micheletti et al. (2003) and the corresponding CFD predictions provided by the Tamburini et al. model (2011a) (along with either SG or MRF technique) for the case of the C=0.15T. Notably, these CFD simulations represent one of the first attempt in the literature to predict the solid distribution in a stirred tank under partial suspension conditions.

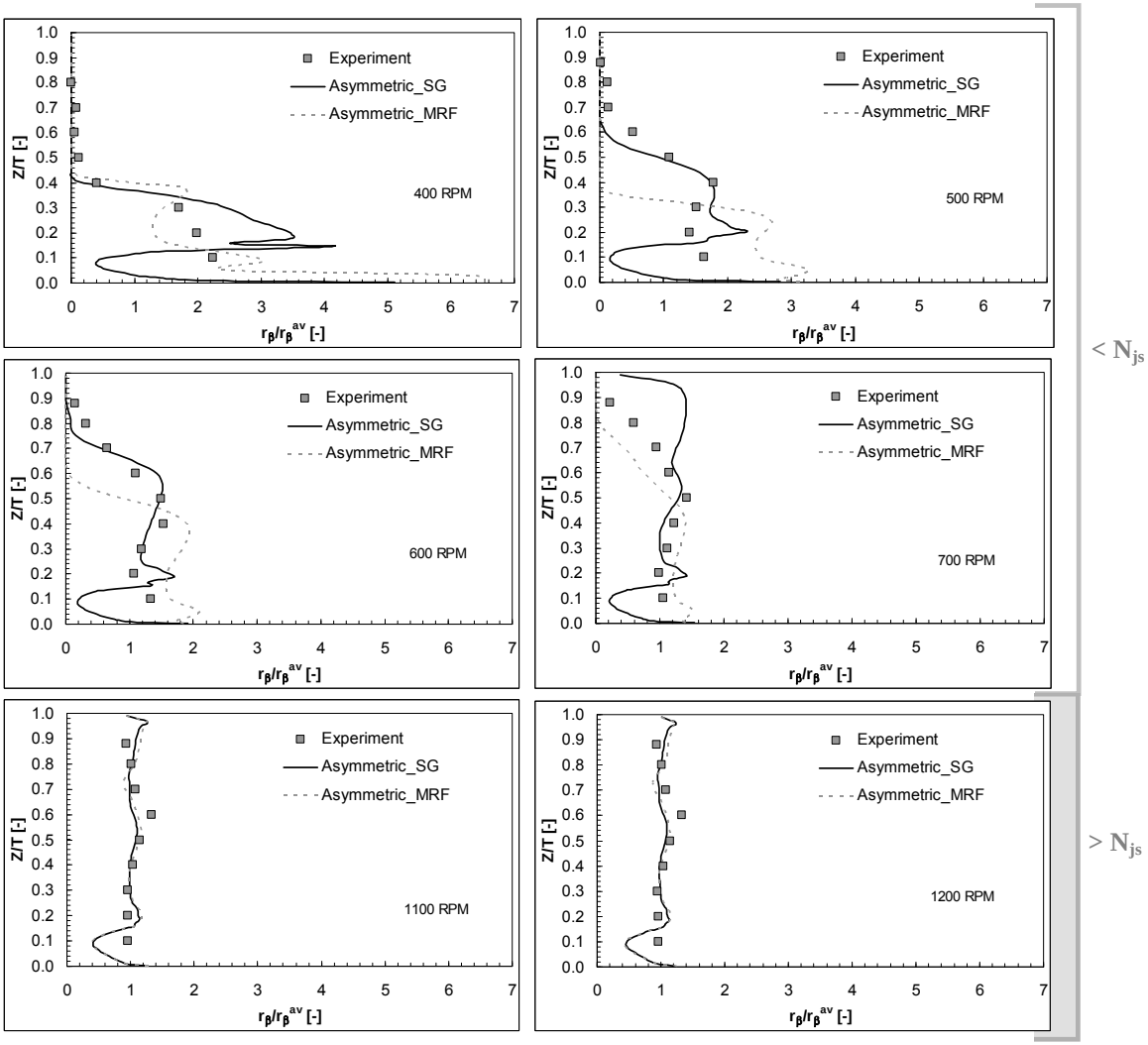

Figure 1: SG/MRF simulations versus experimental (Micheletti et al., 2003) local axial profiles of normalized r_β at some different impeller speeds (impeller placed at C=0.15T).

At 400 RPM (i.e. an N << N_{js}), the model along with both the two impeller techniques provides a good prediction of the experimental profile only above the impeller plane, while slightly disappointing predictions can be observed below the impeller plane. This is allegedly due to the very small distance between the rotating impeller and the sediment, a feature which is clearly difficult to be properly simulated. As a matter of fact, at the same impeller speed and for the case of C=T/3 where the former distance is higher, the experimental profile is very well predicted by the Tamburini et al. model (see Figure2). In particular, the presence of particles near the vessel bottom with a volumetric fraction corresponding to the maximum allowed one (i.e. r_β^{packed} = 0.6) is very well predicted by CFD simulations thus confirming the effectiveness of the ESVC algorithm. At 500 RPM the experimental data are followed fairly well by the SG technique approach especially above the impeller. Conversely, the lowest experimental point (i.e. Z/T=0.1) is not well predicted. This occurrence can be observed at all impeller speeds and it might be due to the very low impeller clearance. As a difference from the SG technique, the model along with the MRF approach fails to predict the experimental data at all heights. A similar behaviour can be observed at 600 RPM where, again, the axial concentration profile apart from the lowest point is fairly predicted by the SG approach. Again, a non negligible difference between the SG and the MRF profiles can be observed especially above the impeller plane: even in this case, the results relevant to the SG technique are in a better agreement with the experimental data. Conversely, at 700 RPM, the model plus the SG approach fails to predict the experimental points in the upper and the lower part of the vessel: in particular an overestimation is observable near the vessel top while an underestimation is found near the vessel bottom. Good predictions were found only at intermediate vessel heights. Only at this impeller speed the MRF approach is in a better agreement with the experiments, although not negligible underestimations are found in the upper part of the vessel. As concerns the unsuspended particle distribution throughout the whole tank, clearly the amount of sediment is reduced as N increases from 400 RPM to 700 RPM. According to Micheletti et al (2003) N_{js} is to be found within the range 800-1000 RPM so that the following cases of Figure1 (i.e. 1100 RPM and 1200 RPM) are relevant to complete suspension conditions. A good agreement between the SG-model prediction and the experimental profile is observable at these impeller speeds. Underestimations of the experimental data can be observed only at Z/T=0.6 and, again, at Z/T=0.1. Notably, the latter under-predictions, formerly seen below the impeller plane for the all the cases, largely reduces at these high N. No difference between the MRF and the SG predictions were found for these two cases thus suggesting that the efficiency of the more simple MRF approach may be linked to the presence of a sediment.

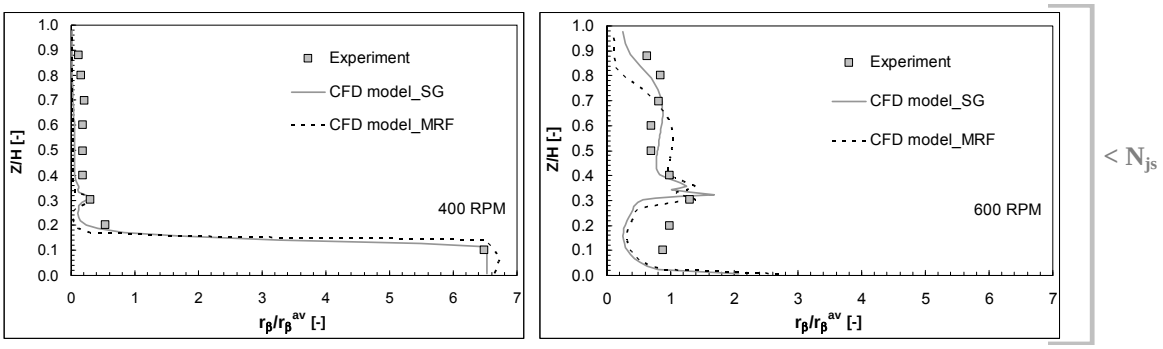

Figure 2: SG/MRF simulations versus experimental (Micheletti et al., 2003) local axial profiles of normalized r_β at some different impeller speeds (impeller placed at C=T/3).

The same comparison is reported in Figure2 for the case of C=T/3: only two impeller speeds are reported for the sake of brevity, other cases can be observed in Tamburini et al. (2013b). Also with this configuration, the Asymmetric model along with the SG algorithm was found to follow quite well the experimental data in all the cases tested (ranging N being below and above N_{js}). Moreover, the SG approach exhibited a better agreement with experiments with respect to the steady state MRF technique as it can be seen, as an example, at 600 RPM in Figure2.
Tamburini et al. (2011a) found that very similar results are provided by SG and MRF in terms of mass fraction of solids resting on the bottom. Conversely differences in the local axial r_β profile were found at all speeds in the present work, as shown in Figure1. Summarizing, it can be stated that for the case of partial suspension conditions, integral data can be predicted with very similar accuracy by SG and MRF simulations, while local information is better predicted by the SG approach. This is not surprising, since the

CFD prediction of local data concerning solid concentration values at different vessel heights allegedly requires a more accurate calculation. As a matter of fact, in accordance with the relevant literature (Panneerselvam et al., 2008), a transient CFD simulation approach based on the fully predictive SG algorithm accounts for the temporal variations in the mixing tank thus providing better predictions of the liquid flow field and solid suspension than the MRF steady state framework.

4.2 Radial profiles of particle concentration

All the axial profiles presented so far refer to a specific radial and azimuthal location: in the literature it is easy to find similar local data, especially when the solids concentration is measured by intrusive techniques making use of a probe. Such local axial data are often extended to the total radial direction. In order to qualitatively evaluate the reliability of this approximation, in Figure3 the local axial profiles already shown in Figure1 are compared with corresponding radially averaged profiles.

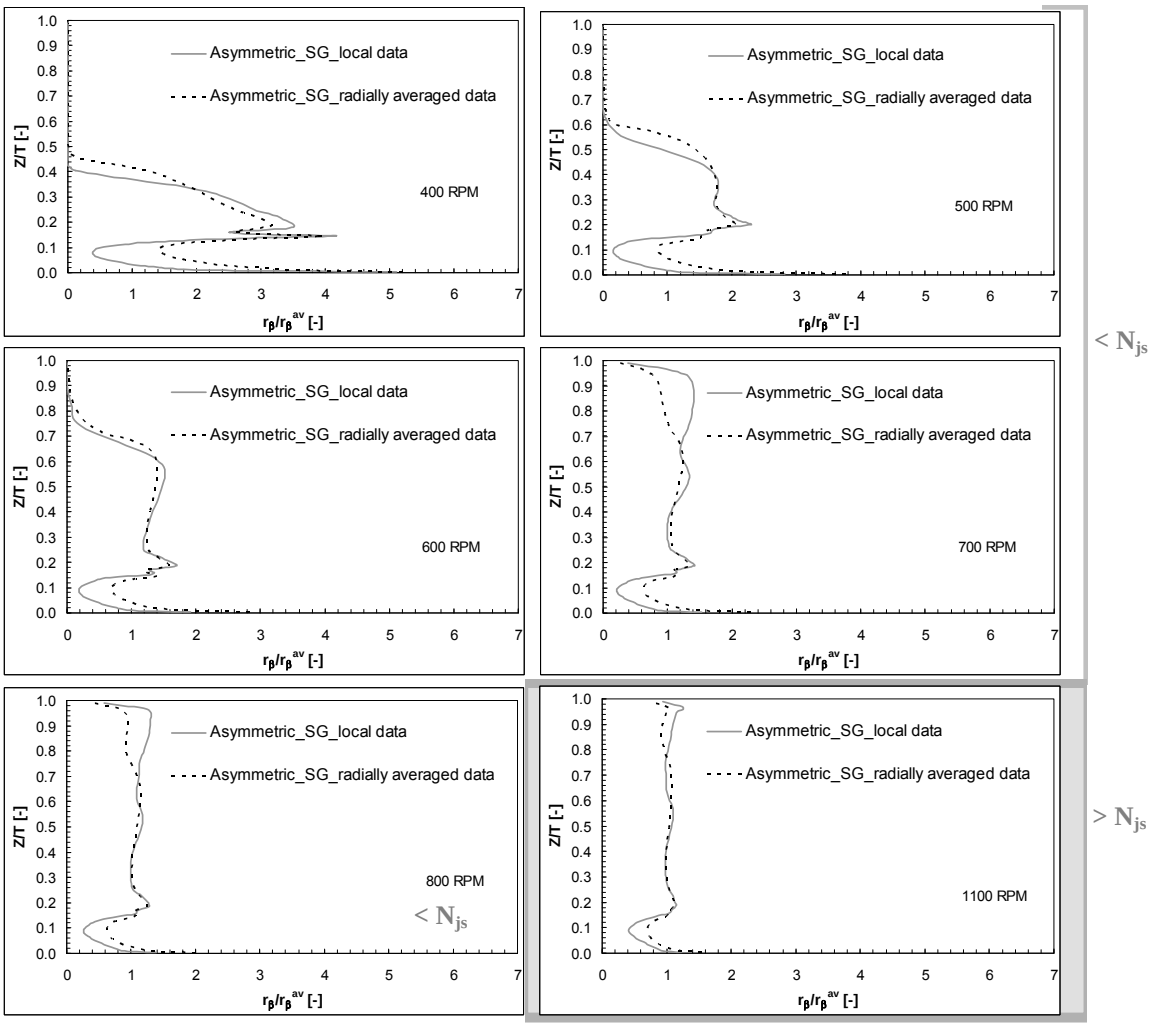

Figure 3: Comparison between local and radially averaged SG axial profiles of r_β (midway between subsequent baffles and at R = 0.35T) at some different impeller speeds (impeller placed at C=0.15T).

At 400 RPM and 500 RPM three different zones separated by two widespread interfaces can be recognized (not shown here): the sediment zone (still solids exhibiting a $r_\beta = r_\beta^{packed}$), the suspension zone and the clear liquid layer zone. As concerns the sediment-suspension interface, at these agitation speeds the sediment is profiled by the liquid flow and exhibits a complex shape. This three-dimensional shape of the sediment-suspension interface makes the assumption of negligible radial and azimuthal r_β gradients unreliable. The local and the radially averaged profiles mainly differ in the proximities of the two widespread interfaces (sediment-suspension and suspension-almost clear liquid layer). As the impeller speeds increases (600, 700 and 800 RPM) the sediment amount decreases thus resulting in a sharper

sediment-suspension interface. This leads to a less pronounced difference between the two profiles in the lower part of the vessel. On the other hand, the single loop flow field due to the low impeller clearance allows the clear liquid layer along with the relevant interface to exist up to intermediate impeller speeds (700 RPM < N < 800 RPM). Also, because of the low impeller clearance, particle velocities are low in the upper part of the vessel thus resulting in a poor radial mixing. Therefore, even in the absence of the sediment-clear liquid layer interface, a significant difference between local and radially averaged profiles can be observed (e.g. at 800 RPM) in the upper part of the tank.
At 1100 RPM, no fillet and clear liquid layer are present, i.e. the suspension occupies the whole vessel volume and the two interfaces are not present: at this high speed, particles move faster and are more homogenously distributed in the vessel thus leading to a slight difference between the two profiles.
Similar considerations could be inferred from the observation of Figure 4 where the impeller clearance is higher (C=T/3). Only some differences can be recognized. As an example at 400 RPM the tank is practically divided in two parts separated by an almost flat interface (Figure 4): the upper part is full of liquid only, the lower one is characterized by the presence of still solids exhibiting a $r_\beta = r_\beta^{packed}$. Under these conditions, radial gradients may be important only in the proximity of the interface between these two zones, while they can be reasonably neglected in the rest of the tank. Due to the higher clearance and to the consequent double loop flow field, the suspension reaches the vessel top at a lower impeller speed with respect to the case with C=0.15T. Moreover, the particles reaching the very top of the vessel move faster in this configuration thus resulting into a better radial mixing (see Figure 4 at 700 RPM)
Summarizing, independently of the impeller to tank relative position it appears that radial gradient of solid concentration may be significant in some cases and in some zones of the vessel under partial suspension conditions where a sediment is present.

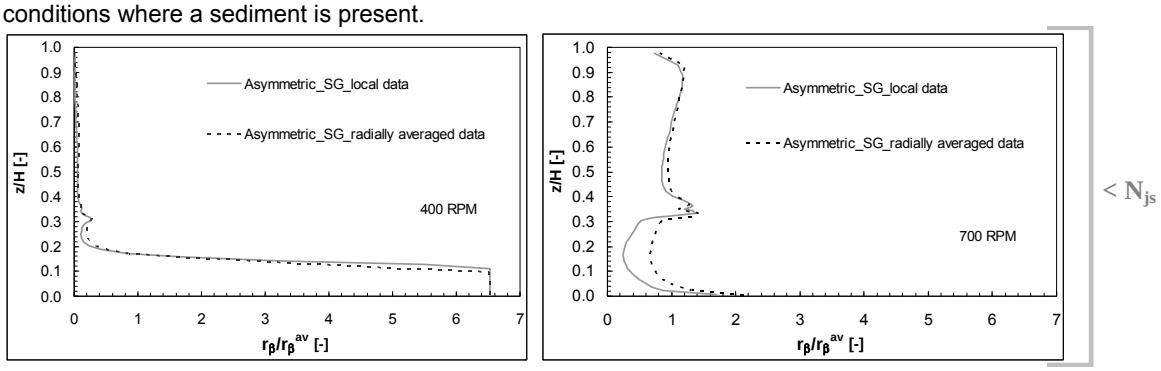

Figure 4: Comparison between local and radially averaged SG axial profiles of r_β (midway between subsequent baffles and at R = 0.35T) at some different impeller speeds (impeller placed at C=T/3).

4.3 Turbulence modelling

Finally, a comparison between two different turbulence modelling approaches was performed: in particular the results, already presented, obtained via the k-ε asymmetric turbulence model were compared with corresponding ones obtained by employing the more common k-ε homogeneous turbulence model. As it can be seen in Figure 5, at low impeller speeds and up to the intermediate value of 600 RPM the homogeneous turbulence model fails to predict the experimental profile. In particular, a large underestimation of the particle distribution degree can be observed. This is likely due to fact that the two phases share the same turbulence kinetic energy *k* and the same dissipation of turbulence kinetic energy ε which are calculated by employing the mixture quantities. In particular, at low to intermediate impeller speeds, when a sediment is present, the mixture velocity used by the turbulence model near the sediment-fluid interface results to be quite lower than that of the liquid phase, thereby leading to compute small velocity gradients, smaller turbulence productions and thus a less intensive turbulence. This effect decreases at higher impeller speeds when the amount of sediment is drastically reduced and the two profiles are closer between each other. However the difference between them is still present up to impeller speeds lower than N_{js}. Notably, at 700-800 RPM the particle distribution degree provided by the *homogeneous k-ε* model is still lower than that of the *asymmetric k-ε* model but in this case it results in a better agreement with experimental data.
A similar yet much less evident behaviour was found for the case of the impeller placed at a clearance C=T/3. For the sake of brevity only the results relevant to two impeller speeds are shown in Figure 6, others can be found in Tamburini et al. (2013b).

These results and the former results (i.e. Figure 5) are in agreement with the findings by Fletcher and Brown (2009) who investigated the solid liquid suspension cloud height limiting their study to the case of intermediate to high impeller speeds: as a matter of fact they found that the *homogeneous* and the *asymmetric k-ε* models provide similar results, but the homogeneous model leads to a lower particle dispersion.

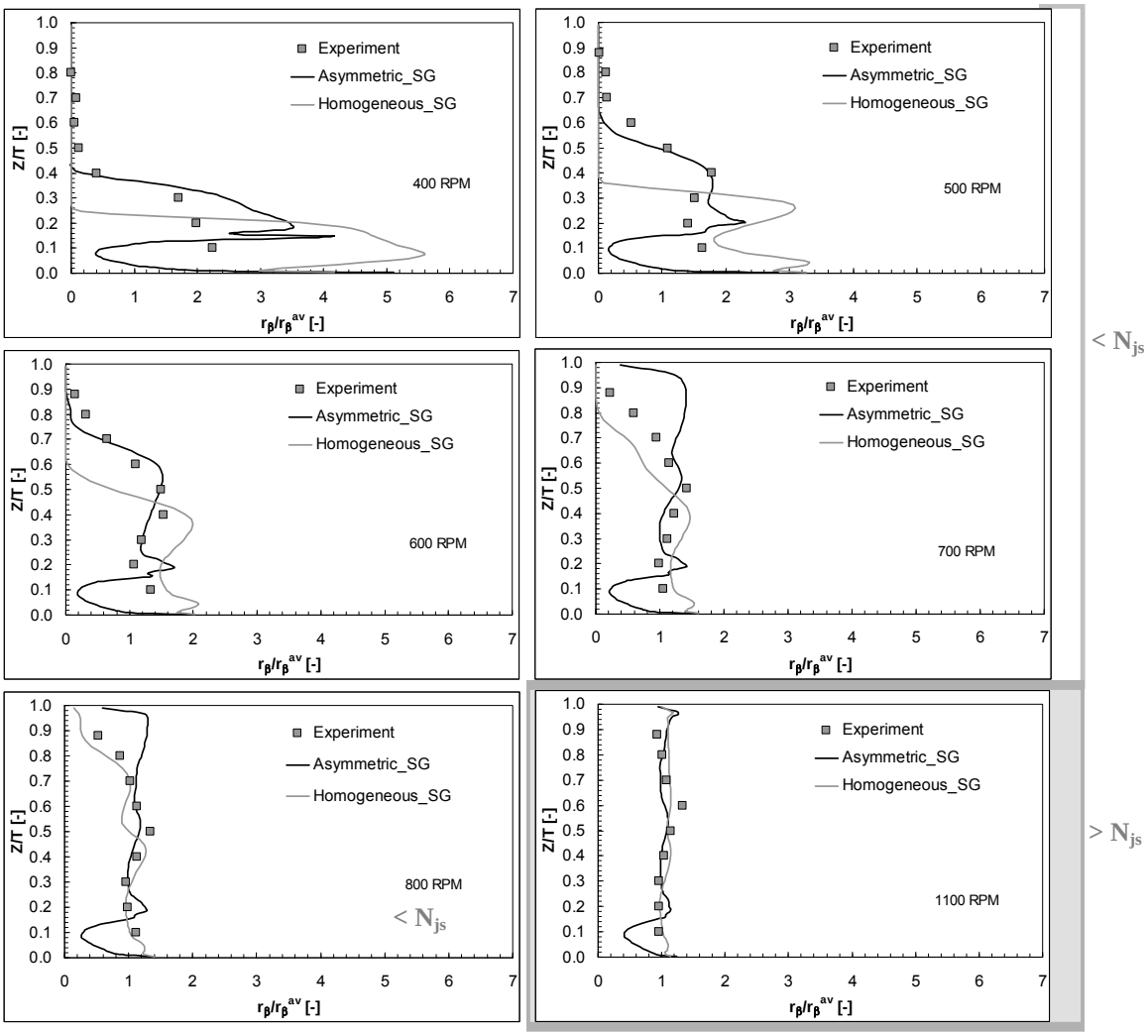

Figure 5: Comparison between two different turbulence modelling approaches: SG local axial profiles of r_β at some different impeller speeds (impeller placed at C= 0.15T).

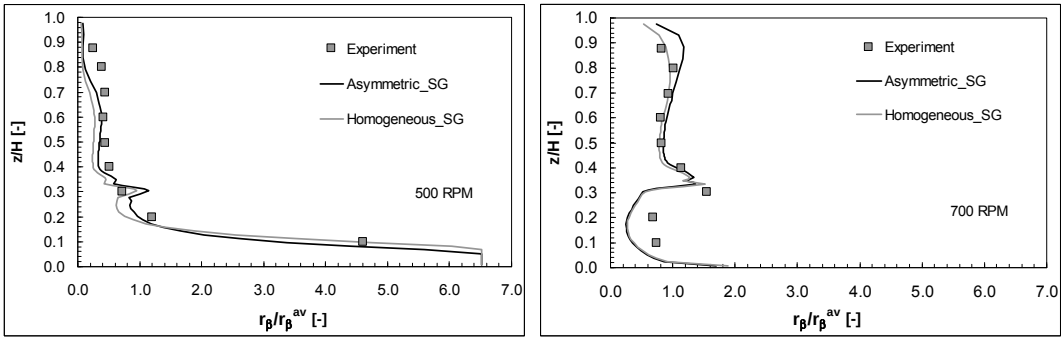

Figure 6: Comparison between two different turbulence modelling approaches: SG local axial profiles of r_β at some different impeller speeds (impeller placed at C= T/3).

5. Conclusions

Reynolds Average Navier Stokes (RANS) simulations of dense solid-liquid suspensions within a flat bottomed vessel stirred by a standard Rushton turbine were performed with a finite volume code by adopting the fully predictive Eulerian-Eulerian Multi Fluid Model in conjunction with the k-ε turbulence model for the continuous (liquid) phase. The specific modelling and numerical details employed were those adopted in Tamburini et al. (2011a) to predict global quantities linked to the particle suspension phenomenon. Here, this model was further tested in order to evaluate its capability of predicting also the three-dimensional particle distribution phenomenon. Both the time-dependent Sliding Grid (SG) method and the steady state Multiple Reference Frame (MRF) technique were used.

Results showed that experimental local axial profiles of solid concentrations (a typical information characterizing the particles distribution) at different impeller speeds ranging from partial to complete suspension conditions can be predicted with a fair accuracy. In particular the transient SG simulation results were found to better predict the experimental data than the steady state MRF simulations.

Although the radial profiles of solid concentrations are often neglected in the literature, the present results showed that this approximation is unjustified in some cases and/or in some zones of the tank, especially under partial suspension conditions in which unsuspended particles are present on the vessel bottom.

As concerns the turbulence modelling, the results found by Fletcher and Brown (2009) (who dealt with experimental cloud height predictions) are confirmed here: the Homogeneous k-ε turbulence model predicts a turbulence less intense than the Asymmetric model thus resulting in a lower particle distribution degree. This effect is enhanced by the presence of a sediment thus resulting in worse predictions for the case of the Homogeneous k-ε turbulence model at very low impeller speeds. The higher the impeller rotational speed the lower the difference between the results relevant to the two approaches.

Summarizing, it can be stated here that a particular attention should be paid when a large amount of motionless particle is present on the vessel bottom thus suggesting that the soundness of all the modelling approaches commonly adopted to manage solid-liquid suspensions in stirred tank should be evaluated at these particular conditions.

References

Barresi A., Baldi G., 1987, Solid dispersion in an agitated vessel, Chem. Eng. Sci., 42, 2949-2956.

Brucato, A., Grisafi, F., Montante, G., 1998, Particle drag coefficients in turbulent fluids, Chem. Eng. Sci., 53, 3295-3314.

Clift, R., Grace, J.R., Weber, M.E., 1978. Bubbles, drops and particles. (Academic Press, New York, San Francisco, London.

Fletcher, D.F., Brown, G.J., 2009. Numerical simulation of solid suspension via mechanical agitation: effect of the modeling approach, turbulence model and hindered settling drag law. Intern. Jour. of Comp. Fluid Dynam. 23, 173-187.

Jafari, R., Chaouhi, J., Tanguy, P.A., 2012. A comprehensive review of just suspended speed in liquid-solid and gas-liquid-solid stirred tank reactors. Int. J. Chem. Reac. Eng. 10, art. no. R1.

Kasat, G. R.; Khopkar, A. R.; Ranade, V. V.; Pandit, A. B, 2008, CFD simulation of liquid-phase mixing in solid-liquid stirred reactor. Chem. Eng. Sci., 63, 3877-3885.

Khopkar, A.R., Kasat, G.R., Pandit, A.B., Ranade, V.V., 2006. Computational Fluid Dynamics simulation of the solid suspension in a stirred slurry reactor. Ind. Eng. Chem. Res. 45, 4416-4428.

Magelli F., Fajner D., Nocentini M., Pasquali G., 1990, Solid distribution in vessels stirred with multiple impellers. Chem. Eng. Sci., 45, 615-625.

Micale G., Brucato A., Grisafi F., Ciofalo M., 1999, Prediction of flow fields in a dual-impeller stirred vessel, AIChE Journal, 45, 445-464.

Micale G., Grisafi F., Rizzuti L., and Brucato A., 2004. CFD Simulation of particle suspension height in stirred vessels. Chem. Eng. Res. Des. 82, 1204-1213.

Micheletti M., Nikiforaki L., Lee K.C., Yianneskis M., 2003, Particle concentration and mixing characteristics of moderate-to-dense solid-liquid suspensions, Ind. Eng. Chem. Res., 42, 6236-6249.

Montante, G. and Magelli, F., 2005. Modelling of solids distribution in stirred tanks: analysis of simulation strategies and comparison with experimental data. Int. Jour Comp. Fluid Dyn. 19, 253-262.

Oldshue, J. Y., 1983, in “Fluid Mixing Technology”, Chapter 5, McGraw-Hill, New York, NY.

Panneerselvam R., Savithri S., Surender G.D., 2008, CFD modeling of gas-liquid-solid mechanically agitated contactor, Chemical Engineering Research Design, 86, 1331-1344.

Rieger, F., Ditl, P., Havelkova, O., 1988. Suspension of solid particles – Concentration profiles and particle layer on the vessel bottom. Proceedings of the 6th European Conference on Mixing, Pavia, Italy, 24-26 May, 251-258.
Shamlou P. A., Koutsakos E., 1989, Solids suspension and distribution in liquids under turbulent agitation, Chemical Engineering Science, 44, 529 – 542.
Tamburini, A., Gentile, L., Cipollina, A., Micale, G., Brucato, A., 2009a. Experimental investigation of dilute solid-liquid suspension in an unbaffled stirred vessels by a novel pulsed laser based image analysis technique, Chemical Engineering Transactions, 17, 531-536.
Tamburini A., Cipollina A., Micale G., Ciofalo M., Brucato A., 2009b, Dense solid–liquid off-bottom suspension dynamics: simulation and experiment, Chem. Eng. Res. Des., 87, 587–597.
Tamburini A., Cipollina A., Micale G., Brucato A., Ciofalo, M., 2011a, CFD simulations of dense solid-liquid suspensions in baffled stirred tanks: predictions of suspension curves, Chem. Eng. J., 178, 324-341.
Tamburini A., Cipollina A., Micale G., 2011b, CFD simulation of solid liquid suspensions in baffled stirred vessels below complete suspension speed, Chemical Engineering Transactions, 24, 1435-1440.
Tamburini A., Brucato A., Cipollina A., Micale G., Ciofalo M., 2012a, CFD predictions of sufficient suspension conditions in solid-liquid agitated tanks, Int. J. Nonlinear Sci. Num. Sim., 13, 427–443.
Tamburini, A. Cipollina A., Micale G., Brucato A., Ciofalo M., 2012b. CFD simulations of dense solid-liquid suspensions in baffled stirred tanks: prediction of the minimum impeller speed for complete suspension. Chem. Eng. J., 193-194, 234–255.
Tamburini A., Cipollina A., Micale G., Brucato A., 2013a, Particle distribution in dilute solid liquid unbaffled tanks via a novel laser sheet and image analysis based technique, Chem. Eng. Sci., 87, 341-358.
Tamburini, A., Cipollina, A., Micale, G., Brucato, A., Ciofalo, M., 2013b, CFD prediction of solid particle distribution in baffled stirred vessels under partial to complete suspension conditions, Chem. Eng. Transactions, 32, 1447-1452.
Tatterson, G. B., 1991. Fluid Mixing and Gas Dispersion in Agitated Tanks. McGraw-Hill: New York.
Van der Westhuizen, A.P. and Deglon, D.A., 2007. Evaluation of solids suspension in a pilot-scale mechanical flotation cell: The critical impeller speed. Minerals Engineering 20, 233-240.
Wang, S., Boger, D.V., Wu, J., 2012. Energy efficient solids suspension in an agitated vessel-water slurry. Chem. Eng. Sci. 74, 233-243.